A SEGMENT-SLIDING RECONSTRUCTION SCHEME FOR PULSED RADAR ECHOES WITH SUB-NYQUIST SAMPLING

Suling Zhang [1], *Feng Xi* [1], *Shengyao Chen* [1], *Yimin D. Zhang* [2], *and Zhong Liu* [1]

[1] Department of Electronic Engineering, Nanjing University of Science and Technology, Nanjing, Jiangsu 210094, China
[2] Department of Electrical & Computer Engineering, Temple University, Philadelphia, PA 19122, USA

ABSTRACT

For radar echoes sampled at sub-Nyquist rates, it is impractical, if not impossible, to recover full-range Nyquist samples because of huge storage and computational loads. By exploiting the banded structure of the measurement matrix, we develop a novel segment-sliding reconstruction (SegSR) scheme to recover the Nyquist samples through low-cost segment-based computations. An important feature of the proposed SegSR scheme is that the measurement sub-matrix in each segment satisfies the restricted isometry property and thus the recovery performance is guaranteed. Because of the segmenting reconstruction, the adjacent segments will introduce interferences for current segment reconstruction. To reduce the effect of such interference, a two-step orthogonal matching pursuit process (TOMPP) algorithm is proposed for improved segment-based reconstructions. The effectiveness of the proposed SegSR with TOMPP is validated by simulations.

Index Terms— Compressive sampling, orthogonal matching pursuit, analog-to-information conversion, segment-sliding reconstruction, sub-Nyquist sampling

1. INTRODUCTION

Analog-to-information conversion (AIC) systems have been proposed to sample wideband signals at sub-Nyquist rates. Among them, random demodulation (RD) [1], [2], random modulator pre-integrator (RMPI) [3], Xampling [4], and quadrature compressed sensing (QuadCS) [5], [6] have received wide attention for radar applications. Theoretical analyses and experimental studies have shown that these AIC systems are efficient for sub-Nyquist acquisition of radar echo signals [7]-[10]. However, in many cases, it is desired to recover the Nyquist samples of radar echoes from sub-Nyquist outputs of AIC systems. This problem refers to the following sparse signal reconstruction,

$$\hat{\boldsymbol{\sigma}} = \arg\min \|\boldsymbol{\sigma}\|_1 \quad \text{s.t.} \quad \mathbf{y} = \boldsymbol{\Phi\Psi\sigma} = \mathbf{A}\boldsymbol{\sigma}, \tag{1}$$

where $\boldsymbol{\sigma}$ is an $N \times 1$ sparse coefficient vector with sparsity (the number of nonzero entries) K, $\mathbf{y}$ is an $M \times 1$ measurement vector, $\boldsymbol{\Phi}$ is an $M \times N$ observation matrix with $M \ll N$, $\boldsymbol{\Psi}$ is an $N \times N$ basis matrix and $\mathbf{A} = \boldsymbol{\Phi\Psi}$ is the yielding $M \times N$ measurement matrix. It has been shown that $\boldsymbol{\sigma}$ can be exactly reconstructed via sparse recovery algorithms [11], if $\mathbf{A}$ satisfies the restricted isometry property (RIP) [12].

However, for radar applications, commonly used sparse reconstruction algorithms may become impractical because of the huge storage and computational requirements. Consider, for example, a radar system with a signal bandwidth of 100 MHz, a pulse width of 10 μs, and a receiving time of 2490 μs. At one-fifth of the Nyquist sampling rate, we need to store a measurement matrix with 99600 rows and 498000 columns, which occupies about 369 GB of memory using the standard IEEE double precision. As a result, the full-range reconstruction is impractical, if not impossible, with the state-of-the-art hardware capabilities. Similar problems also appear in the recovery of sparse signals from streaming measurements [13]-[15]. Several methods [13]-[16] have been proposed to solve such problems. These methods are either unsuitable for radar signal reconstruction or short of theoretical guarantees.

In this paper, we develop a segment-sliding reconstruction (SegSR) scheme to recover full-range pulsed radar echoes from sub-Nyquist samples by the RD system. As revealed in next section, the matrix $\mathbf{A}$ has a banded structure. By taking advantage of this fact, we formulate the measurement sub-matrices which always satisfy the RIP condition, a distinctive characteristic from other segmenting schemes [14]-[16]. Then, we achieve full-range reconstruction by performing sparse reconstruction separately in each segment. Because of the segmenting reconstruction, the adjacent segments will introduce interferences for current segment reconstruction. To suppress the effect of such interferences, we develop a two-step sparse reconstruction approach, which consists of two orthogonal matching pursuit (OMP) processes. Simulation results verify the effectiveness of the proposed SegSR approach.

The remainder of this paper is organized as follows. Section 2 provides the signal model and summarizes the compressive sampling concept for the underlying RD scheme.

This work was supported in part by the National Science Foundation of China under Grants 61171166, 61401210 and 61571228.

Section 3 describes the proposed segment-sliding reconstruction scheme. Numerical results are presented in Section 4. Section 5 concludes this paper.

Notations: Bold letters denote the vectors or matrices. $\|\cdot\|_1$ and $\|\cdot\|_2$ respectively denote the ℓ_1 and ℓ_2 norms of a vector. A vector (matrix) with a set as its subscript denotes the sub-vector (sub-matrix) containing the elements (columns) of the vector (matrix) indexed by the set. $(\cdot)^T$ and $(\cdot)^\dagger$ represent transposition and Moore-Penrose inverse, respectively. $\lceil\cdot\rceil$ and $\lfloor\cdot\rfloor$ respectively denote the ceiling and floor functions.

2. BACKGROUND MATERIALS

2.1. Signal model

Consider a pulsed radar where the baseband signal $s(t)$ has a pulse width of T_p and a bandwidth of $B/2$. Then, for K non-fluctuating point targets, the received echo signal at the baseband can be represented as

$$x(t) = \sum_{k=0}^{K-1} \sigma_k s(t - t_k), \quad t \in [0, T), \tag{2}$$

where t_k and σ_k are the time delay and gain coefficient of the k-th target, respectively, and T refers to the receive time which is usually much larger than T_p, i.e., $T \gg T_p$. For notational succinctness, the background noise is not explicitly presented in the above expression.

Let $\tau_0 = 1/B$ be the Nyquist sampling interval and $N = \lceil T/\tau_0 \rceil$ be the number of Nyquist samples in the receive time T. Assume that target delays are integral multiples of τ_0. Then, $x(t)$ can be expressed in waveform-matched dictionary $\boldsymbol{\psi}(t) = \{\psi_n(t)\}_{n=0}^{N-1}$ with $\psi_n(t) = s(t - n\tau_0)$ as [6],

$$x(t) = \sum_{n=0}^{N-1} \sigma_n \psi_n(t) = \boldsymbol{\psi}(t)\boldsymbol{\sigma}, \tag{3}$$

where $\boldsymbol{\sigma} = [\sigma_0, \sigma_1, \ldots, \sigma_{N-1}]^{\mathrm{T}}$ is a sparse coefficient vector defined over all the possible delay positions. For K targets, there are K nonzero coefficients in $\boldsymbol{\sigma}$. When $K \ll N$, $x(t)$ is K-sparse in $\boldsymbol{\psi}(t)$.

2.2. Compressive sampling of radar echoes

In this section, the principle of compressive sampling is introduced for the RD system, as shown in Fig. 1. The input signal $x(t)$ is first mixed by a pseudorandom ±1 chipping sequence $p(t)$ operating at the chipping rate B_p ($B_p \ge B$), i.e., $p(t) = \pm1$ ($t \in [k/B_p, (k+1)/B_p)$, $k = 0, 1, 2, \ldots$). The mixed signal passes through a low-pass filter to prevent aliasing, and the filtered signal is then sampled. For the accumulated filter, the compressive samples are given by

$$y_m = \int_{(m-1)T_{\mathrm{int}}}^{mT_{\mathrm{int}}} x(t)p(t)dt, \qquad m = 1, 2, \ldots, M, \tag{4}$$

where $T_{\mathrm{int}} = R\tau_0$ is the integration time, and $R > 1$ is an integer referred to as the down sampling rate. During the receive time T, we can acquire $M = \lfloor T/T_{\mathrm{int}} \rfloor$ low-rate samples.

For the waveform-matched dictionary, passing its elements through the RD system yields,

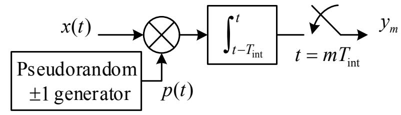

Fig. 1. Structure of the RD system.

$$a_{m,n} = \int_{(m-1)T_{\mathrm{int}}}^{mT_{\mathrm{int}}} \psi_n(t)p(t)dt, \qquad m = 1, 2, \ldots, M. \tag{5}$$

Substituting (3) and (5) into (4) results in

$$y_m = \sum_{n=0}^{N-1} \sigma_n a_{m,n}, \quad m = 1, \ldots, M. \tag{6}$$

Define $\mathbf{y} = [y_1, y_2, \ldots, y_M]^T$, $\mathbf{a}_n = [a_{1,n}, a_{2,n}, \ldots, a_{M,n}]^T$ and $\mathbf{A} = [\mathbf{a}_0, \mathbf{a}_1, \ldots, \mathbf{a}_{N-1}]$. Then, we can express (6) as

$$\mathbf{y} = \sum_{n=0}^{N-1} \sigma_n \mathbf{a}_n = \mathbf{A}\boldsymbol{\sigma}. \tag{7}$$

Here, $\mathbf{y}$ and $\mathbf{A}$ are referred to as the measurement vector and the measurement matrix, respectively. Since $R > 1$, it is clear that $M < N$ and (7) is thus an underdetermined equation. The recovery of the radar echo signal $x(t)$ is equivalent to the reconstruction of the sparse vector $\boldsymbol{\sigma}$.

Note that the RD is a special case of the QuadCS [6] with a zero intermediate frequency. We have proved in [6] that the QuadCS satisfies the RIP for radar signals with flat spectra under the waveform-matched dictionary. Then, the sparse vector $\boldsymbol{\sigma}$ can be exactly reconstructed by solving (1).

As stated in Section 1, directly solving (1) is impractical. Note that $\psi_n(t) = s(t - n\tau_0)$ of $\boldsymbol{\psi}(t)$ has a finite duration of T_p, i.e., $\psi_n(t) = 0$ for $t \notin [n\tau_0, T_p + n\tau_0)$, $n = 0, 1, \ldots, N-1$. Then, it is clear from (5) that the n-th column of the measurement matrix $\mathbf{A}$ takes nonzero values only in finite indexes, i.e., $a_{m,n} = 0$ for $m \le \lfloor n/R \rfloor$ or $m \ge \lceil (T_p + n\tau_0)/T_{\mathrm{int}} \rceil + 1$. Therefore, $\mathbf{A}$ can be described by

$$a_{m,n} = 0, \;\; n/R < m - d \;\; \text{or} \;\; n/R \ge m, \tag{8}$$

where $d = \lceil T_p/T_{\mathrm{int}} \rceil + 1$ for $m = 1, 2, \ldots, M$ and $n = 0, 1, \ldots, N-1$. An example with $B = 10\,\mathrm{MHz}$, $T_p = 0.9\,\mu\mathrm{s}$, and $R = 3$ is shown in Fig. 2 in which $M = 18$ and $N = 45$. It is clearly seen that the matrix $\mathbf{A}$ has a banded structure. By exploiting this structure characteristic, we develop a segment-sliding method where the reconstruction of the vector $\boldsymbol{\sigma}$ is performed in small-size segments.

3. SEGMENT-SLIDING SPARSE RECONSTRUCTION SCHEME

With the banded structure of matrix $\mathbf{A}$, we can perform the reconstruction of the vector $\boldsymbol{\sigma}$ as discussed in [14], [16]. The problem with them is that the resulting measurement sub-matrices cannot be guaranteed to satisfy the RIP conditions. In our development, we take a different way to segment $\boldsymbol{\sigma}$, $\mathbf{y}$ and $\mathbf{A}$ such that the measurement submatrices always satisfy the RIP conditions as long as the full measurement matrix $\mathbf{A}$ does. The segmentation scheme is shown in Fig. 2. The vector $\boldsymbol{\sigma}$ is divided into L overlapping sub-vectors $\tilde{\boldsymbol{\sigma}}^{(l)}$,

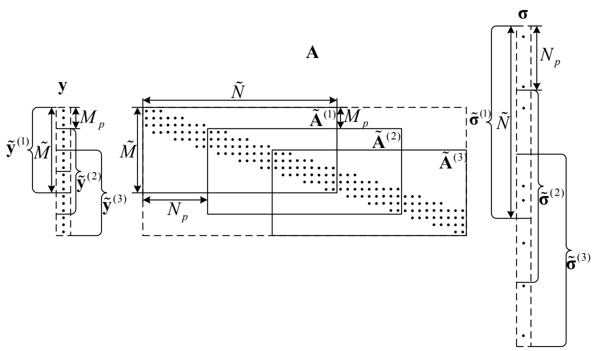

Fig. 2. Schematic illustration of the segmentation.

$$\tilde{\boldsymbol{\sigma}}^{(l)} = \boldsymbol{\sigma}(\tilde{n} : \tilde{n} + \tilde{N} - 1), \quad l = 1,2,\ldots,L, \tag{9}$$

where $\tilde{n} = (l-1)N_p$, $\tilde{N} = SN_p (1 < S < P)$, and $L = P - S$. In (9), we assume that the receive time T is P times the radar pulse width T_p, i.e., $T = PT_p$, and then $N_p = N/P$ is the number of Nyquist samples in a pulse width with P denoting an integer. The segmentation in (9) implies that $\tilde{\boldsymbol{\sigma}}^{(l)}$ is of length SN_p and is sliding down a pulse width in comparison with $\tilde{\boldsymbol{\sigma}}^{(l-1)}$. Let $\tilde{\boldsymbol{\sigma}}_s^{(l)} = \tilde{\boldsymbol{\sigma}}^{(l)}((s-1)N_p : sN_p - 1)$ be the vector of length N_p. We can further express $\tilde{\boldsymbol{\sigma}}^{(l)}$ as $\tilde{\boldsymbol{\sigma}}^{(l)} = [(\tilde{\boldsymbol{\sigma}}_1^{(l)})^T, (\tilde{\boldsymbol{\sigma}}_2^{(l)})^T, \ldots, (\tilde{\boldsymbol{\sigma}}_S^{(l)})^T]^T$. The selection of S depends on the computational capacity and sparsity in the sub-vector $\tilde{\boldsymbol{\sigma}}^{(l)}$. In the following, we assume that sub-vectors $\tilde{\boldsymbol{\sigma}}^{(l)}$ are sparse for all $l = 1,2,\ldots,L$.

Similarly, the measurement vector $\mathbf{y}$ is divided into L overlapping measurement sub-vectors $\tilde{\mathbf{y}}^{(l)}$, expressed as,

$$\tilde{\mathbf{y}}^{(l)} = \mathbf{y}(\tilde{m} : \tilde{m} + \tilde{M} - 1), \quad l = 1,2,\ldots,L, \tag{10}$$

where $\tilde{m} = (l-1)M_p + 1$ and $\tilde{M} = (S+1)M_p$ with $M_p = N/(RP)$ denoting the number of compressive samples within a pulse width.

With the segmentation on $\boldsymbol{\sigma}$ and $\mathbf{y}$, we can formulate an $\tilde{M} \times \tilde{N}$ measurement sub-matrix $\tilde{\mathbf{A}}^{(l)}$ as

$$\tilde{\mathbf{A}}^{(l)} = \mathbf{A}(\tilde{m} : \tilde{m} + \tilde{M} - 1, \tilde{n} : \tilde{n} + \tilde{N} - 1), \; l = 1,2,\ldots,L, \tag{11}$$

by extracting the columns and rows of $\mathbf{A}$ corresponding to $\tilde{\boldsymbol{\sigma}}^{(l)}$ and $\tilde{\mathbf{y}}^{(l)}$ (refer to Fig. 2). Following the partitioning of $\tilde{\boldsymbol{\sigma}}^{(l)}$, we can express $\tilde{\mathbf{A}}^{(l)}$ as $\tilde{\mathbf{A}}^{(l)} = [\tilde{\mathbf{A}}_1^{(l)}, \tilde{\mathbf{A}}_2^{(l)}, \ldots, \tilde{\mathbf{A}}_S^{(l)}]$ with $\tilde{\mathbf{A}}_s^{(l)} = \tilde{\mathbf{A}}^{(l)}(1 : \tilde{M}, (s-1)N_p : sN_p - 1)$.

From (9), (10) and (11), we have

$$\tilde{\mathbf{y}}^{(l)} = \begin{cases} \tilde{\mathbf{A}}^{(l)}\tilde{\boldsymbol{\sigma}}^{(l)} + \underset{\sim}{\tilde{\mathbf{A}}}^{(l+1)}\tilde{\boldsymbol{\sigma}}_S^{(l+1)}, & l = 1, \\ \underset{\sim}{\tilde{\mathbf{A}}}^{(l-1)}\tilde{\boldsymbol{\sigma}}_1^{(l-1)} + \tilde{\mathbf{A}}^{(l)}\tilde{\boldsymbol{\sigma}}^{(l)} + \underset{\sim}{\tilde{\mathbf{A}}}^{(l+1)}\tilde{\boldsymbol{\sigma}}_S^{(l+1)}, & l = 2,3,\ldots,L-1, \\ \underset{\sim}{\tilde{\mathbf{A}}}^{(l-1)}\tilde{\boldsymbol{\sigma}}_1^{(l-1)} + \tilde{\mathbf{A}}^{(l)}\tilde{\boldsymbol{\sigma}}^{(l)}, & l = L, \end{cases} \tag{12}$$

where

$$\underset{\sim}{\tilde{\mathbf{A}}}^{(l-1)} = \begin{bmatrix} \tilde{\mathbf{A}}_1^{(l-1)}(M_p + 1 : \tilde{M}, 0 : N_p - 1) \\ \mathbf{0}_{M_p \times N_p} \end{bmatrix}, \tag{13}$$

$$\underset{\sim}{\tilde{\mathbf{A}}}^{(l+1)} = \begin{bmatrix} \mathbf{0}_{M_p \times N_p} \\ \tilde{\mathbf{A}}_S^{(l+1)}(1 : \tilde{M} - M_p, 0 : N_p - 1) \end{bmatrix}. \tag{14}$$

It is observed in (12) that $\tilde{\mathbf{y}}^{(l)}$ is generally related to three sub-vectors $\tilde{\boldsymbol{\sigma}}_1^{(l-1)}$, $\tilde{\boldsymbol{\sigma}}^{(l)}$, and $\tilde{\boldsymbol{\sigma}}_S^{(l+1)}$. The terms $\underset{\sim}{\tilde{\mathbf{A}}}^{(l-1)}\tilde{\boldsymbol{\sigma}}_1^{(l-1)}$ and $\underset{\sim}{\tilde{\mathbf{A}}}^{(l+1)}\tilde{\boldsymbol{\sigma}}_S^{(l+1)}$ are due to the contributions of $\tilde{\boldsymbol{\sigma}}_1^{(l-1)}$ and $\tilde{\boldsymbol{\sigma}}_S^{(l+1)}$, respectively. Define

$$\underline{\tilde{\mathbf{y}}}^{(l)} = \begin{cases} \tilde{\mathbf{y}}^{(l)}, & l = 1, \\ \tilde{\mathbf{y}}^{(l)} - \underset{\sim}{\tilde{\mathbf{A}}}^{(l-1)}\hat{\tilde{\boldsymbol{\sigma}}}_1^{(l-1)}, & l = 2,3,\ldots,L, \end{cases} \tag{15}$$

where $\hat{\tilde{\boldsymbol{\sigma}}}_1^{(l-1)}$ is the estimate of $\tilde{\boldsymbol{\sigma}}_1^{(l-1)}$. Moreover, define

$$\underline{\tilde{\mathbf{n}}}^{(l)} = \begin{cases} \underset{\sim}{\tilde{\mathbf{A}}}^{(l+1)}\tilde{\boldsymbol{\sigma}}_S^{(l+1)}, & l = 1, \\ \underset{\sim}{\tilde{\mathbf{A}}}^{(l-1)}\Delta\tilde{\boldsymbol{\sigma}}_1^{(l-1)} + \underset{\sim}{\tilde{\mathbf{A}}}^{(l+1)}\tilde{\boldsymbol{\sigma}}_S^{(l+1)}, & l = 2,3,\ldots,L-1, \\ \underset{\sim}{\tilde{\mathbf{A}}}^{(l-1)}\Delta\tilde{\boldsymbol{\sigma}}_1^{(l-1)}, & l = L. \end{cases} \tag{16}$$

where $\Delta\tilde{\boldsymbol{\sigma}}_1^{(l-1)} = \tilde{\boldsymbol{\sigma}}_1^{(l-1)} - \hat{\tilde{\boldsymbol{\sigma}}}_1^{(l-1)}$ is the error between $\tilde{\boldsymbol{\sigma}}_1^{(l-1)}$ and $\hat{\tilde{\boldsymbol{\sigma}}}_1^{(l-1)}$. Then, we have a general form of compressive measurements in the presence of noise as

$$\underline{\tilde{\mathbf{y}}}^{(l)} = \tilde{\mathbf{A}}^{(l)}\tilde{\boldsymbol{\sigma}}^{(l)} + \underline{\tilde{\mathbf{n}}}^{(l)}, \; l = 1,2,\ldots,L. \tag{17}$$

Note that $\underline{\tilde{\mathbf{n}}}^{(l)}$ stems from the estimation error in the previous segment and the partial measurement in the subsequent segment. For convenience, we refer to $\underline{\tilde{\mathbf{n}}}^{(l)}$ as the *virtual noise* sub-vector and $\underset{\sim}{\tilde{\mathbf{A}}}^{(l-1)}\Delta\tilde{\boldsymbol{\sigma}}_1^{(l-1)}$ and $\underset{\sim}{\tilde{\mathbf{A}}}^{(l+1)}\tilde{\boldsymbol{\sigma}}_S^{(l+1)}$ as the forward and backward virtual noise, respectively. Their effect on the reconstruction of $\tilde{\boldsymbol{\sigma}}^{(l)}$ is simulated in Section 4. Similarly, we refer to $\underline{\tilde{\mathbf{y}}}^{(l)}$ as a *virtual* measurement sub-vector.

It becomes clear that the large-scale reconstruction (1) is now decomposed into L small-scale ones (17). As such, we can robustly reconstruct $\tilde{\boldsymbol{\sigma}}^{(l)}$ by solving the constrained optimization problem

$$\hat{\tilde{\boldsymbol{\sigma}}}^{(l)} = \arg\min \left\|\tilde{\boldsymbol{\sigma}}^{(l)}\right\|_1 \;\; \text{s.t.} \;\; \left\|\underline{\tilde{\mathbf{y}}}^{(l)} - \tilde{\mathbf{A}}^{(l)}\tilde{\boldsymbol{\sigma}}^{(l)}\right\|_2 \le \eta^{(l)}, \tag{18}$$

in which $\left\|\underline{\tilde{\mathbf{n}}}^{(l)}\right\|_2 \le \eta^{(l)}$. We name the method as segment-sliding sparse reconstruction (SegSR), which is summarized as Algorithm 1.

Algorithm 1. SegSR Scheme

Input: S, M_p, N_p, $\tilde{M}$, $\tilde{N}$ and L
Output: Estimated sparse vector $\hat{\boldsymbol{\sigma}}$
Steps:

1) Initialize $l = 1$.
2) Extract the $\tilde{M} \times 1$ measurement sub-vector $\tilde{\mathbf{y}}^{(l)}$ and the $\tilde{M} \times \tilde{N}$ measurement sub-matrix $\tilde{\mathbf{A}}^{(l)}$.
3) Calculate the virtual measurement sub-vector $\underline{\tilde{\mathbf{y}}}^{(l)}$ by (15).
4) Solve (18) and obtain the estimate $\hat{\tilde{\boldsymbol{\sigma}}}^{(l)}$ of $\tilde{\boldsymbol{\sigma}}^{(l)}$.
5) Let $l = l + 1$. If $l > L$, go to Step 6); otherwise, generate the $\tilde{M} \times \tilde{N}$ sub-matrix $\underset{\sim}{\tilde{\mathbf{A}}}^{(l-1)}$ by (13), extract the sub-vector $\hat{\tilde{\boldsymbol{\sigma}}}_1^{(l-1)}$ from the estimated $\hat{\tilde{\boldsymbol{\sigma}}}^{(l-1)}$ and go to Step 2).
6) Estimate the sparse vector $\boldsymbol{\sigma}$ as
$$\begin{cases} \hat{\boldsymbol{\sigma}}((l-1)N_p : lN_p - 1) = \hat{\tilde{\boldsymbol{\sigma}}}_1^{(l)}, & l = 1,\ldots,L-1, \\ \hat{\boldsymbol{\sigma}}((l-1)N_p : N - 1) = \hat{\tilde{\boldsymbol{\sigma}}}^{(L)}, & l = L. \end{cases}$$

Note that each column of $\tilde{\mathbf{A}}^{(l)}$ completely contains all nonzero elements of the corresponding column of $\mathbf{A}$, and then the sub-matrix $\tilde{\mathbf{A}}^{(l)}$ in (17) satisfies the RIP, which is different from other formulations [14], [16].

Solving (18) is one of the major steps in the proposed SegSR scheme. From (16), we note that the forward and

Algorithm 2. TOMPP

Input: $\underline{\tilde{\mathbf{y}}}^{(l)}$, $\tilde{\mathbf{A}}^{(l)}$, N_p, $\tilde{N}$, $\hat{\tilde{\boldsymbol{\sigma}}}^{(l-1)}$, threshold parameters ζ_1 and ζ_2 ($\zeta_2 < \zeta_1$)

Output: Estimated sparse sub-vector $\hat{\tilde{\boldsymbol{\sigma}}}^{(l)}$

Steps:

1) Initialize the index set $\Lambda^{[0]}$ as the known support in the l-th segment estimate, $\Lambda^{[0]} = \mathrm{support}\left(\hat{\tilde{\boldsymbol{\sigma}}}^{(l-1)}(N_p : \tilde{N}-1)\right)$; the residual $\tilde{\mathbf{r}}^{[0]} = \left(\mathbf{I} - \mathbf{P}_0\right)\underline{\tilde{\mathbf{y}}}^{(l)}$, where $\mathbf{P}_0 = \tilde{\mathbf{A}}^{(l)}_{\Lambda^{[0]}}\left(\tilde{\mathbf{A}}^{(l)}_{\Lambda^{[0]}}\right)^{\dagger}$ denotes the projection onto the linear space spanned by the columns of $\tilde{\mathbf{A}}^{(l)}_{\Lambda^{[0]}}$. Let $i = 1$.
2) Find the column of $\tilde{\mathbf{A}}^{(l)}$ that has the highest correlation with the residual $\tilde{\mathbf{r}}^{[i-1]}$, i.e.,
$$\lambda^{[i]} = \arg\max_{j=0,1,\ldots,\tilde{N}-1}\left|\left\langle \tilde{\mathbf{a}}^{(l)}_j, \tilde{\mathbf{r}}^{[i-1]}\right\rangle\right|,$$
and update the index set $\Lambda^{[i]} = \Lambda^{[i-1]} \bigcup \left\{\lambda^{[i]}\right\}$.
3) Update the residual as $\tilde{\mathbf{r}}^{[i]} = \left(\mathbf{I} - \mathbf{P}_i\right)\underline{\tilde{\mathbf{y}}}^{(l)}$.
4) Let $i = i+1$. If $\left\|\tilde{\mathbf{r}}^{[i-1]}\right\|_2 - \left\|\tilde{\mathbf{r}}^{[i]}\right\|_2 \le \zeta_1$, go to Step 5); otherwise, return to Step 2).
5) For columns $0 \sim \tilde{N} - N_p - 1$ of $\tilde{\mathbf{A}}^{(l)}$, find the column that has the highest correlation with the residual $\tilde{\mathbf{r}}^{[i-1]}$, i.e.,
$$\lambda^{[i]} = \arg\max_{j=0,1,\ldots,\tilde{N}-N_p-1}\left|\left\langle \tilde{\mathbf{a}}^{(l)}_j, \tilde{\mathbf{r}}^{[i-1]}\right\rangle\right|,$$
and update the index set $\Lambda^{[i]} = \Lambda^{[i-1]} \bigcup \left\{\lambda^{[i]}\right\}$.
6) Update the residual as $\tilde{\mathbf{r}}^{[i]} = \left(\mathbf{I} - \mathbf{P}_i\right)\underline{\tilde{\mathbf{y}}}^{(l)}$.
7) If $\left\|\tilde{\mathbf{r}}^{[i-1]}\right\|_2 - \left\|\tilde{\mathbf{r}}^{[i]}\right\|_2 \le \zeta_2$, go to Step 8); otherwise, let $i = i+1$ and return to Step 5).
8) Compute the estimate $\hat{\tilde{\boldsymbol{\sigma}}}^{(l)}$ as $\hat{\tilde{\boldsymbol{\sigma}}}^{(l)}_{\Lambda^{[i]}} = \left(\tilde{\mathbf{A}}^{(l)}_{\Lambda^{[i]}}\right)^{\dagger}\underline{\tilde{\mathbf{y}}}^{(l)}$.

backward virtual noise exists only in the range of $[1:M_p]$ ($[\tilde{M} - M_p + 1 : \tilde{M}]$), and the backward virtual noise level is generally much higher than that of the forward virtual noise. Then we can utilize two OMP processes to improve the reconstruction. The first OMP process with threshold ζ_1 obtains a rough estimate (Steps 2-4 in Algorithm 2) derived for the whole virtual noise, and the second one with threshold ζ_2 (Steps 5-7 in Algorithm 2) refines the estimate for sparse coefficients lied in $[0:\tilde{N} - N_p - 1]$. The resulting algorithm is referred to as two-step OMP process (TOMPP). In addition, there exists a partial overlap between two consecutive segments of the sparse vector $\boldsymbol{\sigma}$. Then the partially known support (PKS) from the previous segment can be incorporated into the initialization of the first OMP process in the current segment (Step 1 in Algorithm 2), which further improves the reconstruction performance.

4. SIMULATION RESULTS

In this section, we evaluate the performance of the proposed SegSR scheme through several simulation experiments. Without special statements, 500 realizations are conducted and the averaged results are presented. The reconstruction error and the running time of the SegSR scheme with OMP-PKS [17] and TOMPP are presented and the relative reconstruction error $E_r = \|\hat{\boldsymbol{\sigma}} - \boldsymbol{\sigma}\|_2 / \|\boldsymbol{\sigma}\|_2$ is taken as the criterion for performance evaluation.

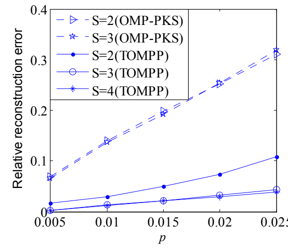

Fig. 3. Relative reconstruction error.

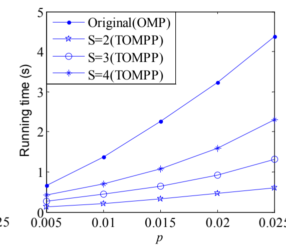

Fig. 4. Running time.

We consider a linear frequency modulated (LFM) pulse signal with bandwidth $B = 100$ MHz and pulse width $T_p = 10$ μs. To make a comparison with direct reconstruction, we set the receive time $T = 100$ μs such that the measurement matrix is of a moderate size. For the RD system, we set the chipping rate to be $B_p = 100$ MHz and the integration time to be $T_{\mathrm{int}} = 0.05$ μs. For echo model (2), we assume that the amplitudes follow a uniform distribution in $(0,1]$, and the time delays are randomly chosen in resolution grids. Furthermore, it is assumed that the elements of the coefficient vector $\boldsymbol{\sigma}$ take a nonzero value with a probability p.

Fig. 3 shows the relative reconstruction error versus p for different values of S in the noiseless case. The OMP results obtained from direct solving (1) are not shown here, because they derive much smaller errors in the noise-free case. It is seen that the relative reconstruction errors by the TOMPP are much lower than those obtained from the OMP-PKS. For the parameters being studied, the relative reconstruction errors by the TOMPP do not significantly change when S is larger than 3.

We now use CPU time to illustrate the running time. The simulation is performed using MATLAB 2011b in a PC with 3.1 GHz Intel core i5-2400 processor and 4 GB RAM. The running times of the SegSR scheme with TOMPP and the original direct reconstruction by OMP are given in Fig. 4. It is clear that the TOMPP is much faster than the OMP. It should be noted that the simulations are only illustrative for a moderate size example. In fact, the TOMPP solves large-scale reconstruction problems which cannot be solved directly by the OMP. Note that the running time of TOMPP increases as S increases. Considering the reconstruction error and the running time, $S = 3$ is chosen in our simulations.

5. CONCLUSION

In this paper, we have developed a SegSR scheme to recover full-range pulsed radar echoes from the sub-Nyquist samples. The SegSR scheme decomposes a large-scale reconstruction problem into a series of small-scale ones, and all the measurement sub-matrices satisfy the RIP conditions such that the recovery performance can be guaranteed. Although developed from RD, the SegSR scheme can be applied to other AIC systems in which the measurement matrices have a similar structure.

6. REFERENCES

[1] S. Kirolos, J. Laska, M. Wakin, M. Duarte, D. Baron, T. Ragheb, Y. Massoud, and R. Baraniuk, "Analog-to-information conversion via random demodulation," in *Proc. IEEE Dallas Circuits and Systems Workshop (DCAS)*, Dallas, TX, 2006, pp. 71-74.

[2] J. A. Tropp, J. N. Laska, M. F. Duarte, J. K. Romberg, and R. G. Baraniuk, "Beyond Nyquist: Efficient sampling of sparse bandlimited signals," *IEEE Trans. Inf. Theory*, vol. 56, no. 1, pp. 520-544, 2010.

[3] S. Becker, *Practical Compressed Sensing: Modern Data Acquisition and Signal Processing*, Ph.D. dissertation, California Institute of Technology, Pasadena, California, 2011.

[4] M. Mishali, Y. C. Eldar, and A. J. Elron, "Xampling: Signal acquisition and processing in union of subspaces," *IEEE Trans. Signal Process.*, vol. 59, no. 10, pp. 4719-4734, 2011.

[5] F. Xi, S. Chen, and Z. Liu, "Quadrature compressive sampling for radar echo signals," in *Proc. Int. Conf. on Wireless Communications and Signal Processing (WCSP)*, Nanjing, China, 2011, pp. 1-5.

[6] F. Xi, S. Chen, and Z. Liu, "Quadrature compressive sampling for radar signals," *IEEE Trans. Signal Process.*, vol. 62, no. 11, pp. 2787-2802, 2014.

[7] J. Yoo, C. Turnes, E. B. Nakamura, C. K. Le, S. Becker, E. A. Sovero, M. B. Wakin, M. C. Grant, J. Romberg, A. Emami-Neyestanak, and E. Candès, "A compressed sensing parameter extraction platform for radar pulse signal acquisition," *IEEE J. Emerging Sel. Top. Circuits Syst.*, vol. 2, no. 3, pp. 626-638, 2012.

[8] C. Liu, F. Xi, S. Chen, Y. D. Zhang, and Z. Liu, "Pulse-doppler signal processing with quadrature compressive sampling," *IEEE Trans. Aerosp. Electron. Syst.*, vol. 51, no. 2, pp. 1217-1230, 2015.

[9] O. Bar-Ilan and Y. C. Eldar, "Sub-Nyquist radar via Doppler focusing," *IEEE Trans. Signal Process.*, vol. 62, no. 7, pp. 1796-1811, 2014.

[10] I. Kyriakides, "Adaptive compressive sensing and processing of delay-Doppler radar waveforms," *IEEE Trans. Signal Process.*, vol. 60, no. 2, pp. 730-739, 2012.

[11] M. Fornasier, "Numerical methods for sparse recovery," *Radon Series Comp. Appl. Math.*, vol. 9, pp. 1-110, 2010.

[12] E. Candès and T. Tao, "Decoding by linear programming," *IEEE Trans. Inf. Theory*, vol. 51, no.12, pp. 4203-4215, 2005.

[13] N. M. Freris, O. Öçal, and M. Vetterli, "Compressed sensing of streaming data," in *Proc. 51st Annu. Allerton Conf. Commun., Contr., Comput.*, Monticello, IL, 2013, pp. 1242-1249.

[14] T. B. Petros and M. S. Asif, "Compressive sensing for streaming signals using the streaming greedy pursuit," in *Proc. 2010 Military Communications Conference (MILCOM 2010)*, San Jose, CA, 2010, pp. 1205-1210.

[15] M. S. Asif and J. Romberg, "Sparse recovery of streaming signals using ℓ_1-homotopy," *IEEE Trans. Signal Process.*, vol. 62, no. 16, pp. 4209-4223, 2014.

[16] S. Qin, Y. D. Zhang, Q. Wu, and M. G. Amin, "Large-scale sparse reconstruction through partitioned compressive sensing," in *Proc. 19th Int. Conf. on Digital Signal Processing (DSP 2014)*, Hong Kong, China, 2014, pp. 837-840.

[17] R. E. Carrillo, L. F. Polania, and K. E. Barner, "Iterative algorithms for compressed sensing with partially known support," in *Proc. IEEE Int. Conf. on Acoustics, Speech, and Signal Processing (ICASSP)*, Dallas, TX, 2010, pp. 3654-3657.